Available online at www.sciencedirect.com
ScienceDirect
Developmental Biology 316 (2008) 36–49
DEVELOPMENTAL BIOLOGY
www.elsevier.com/developmentalbiology

Tjp3/zo-3 is critical for epidermal barrier function in zebrafish embryos

Tanja K. Kiener, Inna Selptsova-Friedrich [1], Walter Hunziker *

*Epithelial Cell Biology Laboratory, Institute of Molecular and Cell Biology, A*STAR (Agency for Science Technology and Research), Singapore 138673, Singapore*

Received for publication 8 August 2007; revised 11 December 2007; accepted 30 December 2007
Available online 26 January 2008

Abstract

TJP3/ZO-3 is a scaffolding protein that tethers tight junction integral membrane proteins to the actin cytoskeleton and links the conserved Crumbs polarity complex to tight junctions. The physiological function of TJP3/ZO-3 is not known and mice lacking TJP3/ZO-3 show no apparent phenotype. Here we show that Tjp3/Zo-3 is a component of tight junctions present in the enveloping cell layer of zebrafish embryos. Silencing *tjp3/zo-3* using morpholinos leads to edema, loss of blood circulation and tail fin malformations in the embryos. The ultrastructure of tight junctions of the enveloping cell layer is disrupted, without affecting the asymmetric distribution of plasma membrane proteins. Morphants show a loss of the epidermal barrier, as assessed by an increased permeability of the enveloping cell layer to low molecular weight tracers and a higher sensitivity of the embryos to osmotic stress. Subjecting wild-type embryos to osmotic stress mimicks the morphant phenotype, consistent with the phenotype being a direct consequence of failed osmoregulation. Thus, Tjp3/Zo-3 is critical for barrier function of the enveloping cell layer and osmoregulation in early stages of zebrafish development.

Keywords: Tight junction; Zonula occludens; Enveloping cell layer; Epidermis; Kidney; Diffusion barrier; Osmoregulation

Introduction

Tight junctions (TJs) are important components of epithelial tissues where they are required for barrier function, epithelial cell polarity and signaling events in response to cell–cell contact (Anderson et al., 2004; Matter and Balda, 2007; Tsukita et al., 2001). Structurally, TJs are composed of integral membrane proteins such as claudins and occludin, which are tethered to the actin cytoskeleton via scaffold or adaptor proteins (Gonzalez-Mariscal et al., 2003; Tsukita et al., 2001; Van Itallie and Anderson, 2006). Among the best-characterized scaffold proteins are three closely related members of the membrane-associated guanylate kinase-like (MAGUK) protein superfamily, TJP1/ZO-1, TJP2/ZO-2 and TJP3/ZO-3 (Gonzalez-Mariscal et al., 2000). An increasing number of proteins that interact with these adaptors have been described, but the role of individual members of the TJP/ZO protein family in the function of TJs remains unclear (Gonzalez-Mariscal et al., 2000). In addition, most of the functional studies to date have focused on tissue culture cell lines such as renal MDCK or mammary EpH4 cells and the relevance of these proteins in the physiology of living organisms is poorly understood.

Analysis of the role of ZO proteins in cell polarity, TJ barrier function and signaling pathways using tissue culture cells have been conflicting, perhaps reflecting cell type differences and/or the extent of protein depletion, depending on whether gene inactivation was achieved by homologous recombination or silencing. Only minor effects on the assembly kinetics and functions of TJs were detected following the ablation of TJP1/ZO-1 by homologous recombination in Eph4 mammary epithelial cells (Umeda et al., 2004) or RNA interference in MDCK renal epithelial cells (McNeil et al., 2006). Silencing of ZO-2 alone also had no discernable effect on barrier function or polarity of MDCK (McNeil et al., 2006) and EpH4 (Umeda

Abbreviations: AJ, adherens junction; GUK, guanylate kinase; MO, morpholino oligonucleotide; MAGUK, membrane-associated guanylate kinase-like; PCR, polymerase chain reaction; PDZ, PSD95/Dlg/ZO-1; S.E.M., standard error of the mean; siRNA, small interfering RNA; SH3, Src homology 3; TEM, transmission electron microscopy; TJ, tight junction; TJP, tight junction protein; WT, wild-type; ZO, zonula occludens.

* Corresponding author.
E-mail address: hunziker@imcb.a-star.edu.sg (W. Hunziker).
[1] Present address: Vario Health Institute, Edith Cowan University, Joondalup Campus, Joondalup WA 6027, Perth, Australia.

0012-1606/$ - see front matter © 2008 Elsevier Inc. All rights reserved.
doi:10.1016/j.ydbio.2007.12.047

et al., 2006) cells, but a recent study described effects on both functions in siRNA treated MDCK cells. *ZO-3*-null cell lines derived from mice with a targeted inactivation of the *ZO-3* gene, showed no obvious phenotype (Adachi et al., 2006). These findings, while sometimes conflicting, suggest that the lack of a single ZO protein may be largely dispensable for TJ structure and function. Only recently have the physiological roles of these proteins been explored using animal models. Surprisingly given the epithelial cell specific expression of *ZO-3*, mice carrying an inactivated *ZO-3* gene present with no apparent phenotype (Adachi et al., 2006; Xu et al., 2008).

Recent evidence supports the notion that when compared to mammals, teleosts may have a more complex repertoire of TJ components, perhaps reflecting the need to maintain osmotic balance in the aqueous environment in which they live. In fugu, for example, claudin genes have undergone an unprecedented expansion, resulting in the expression of over 55 different claudin genes in different tissues or developmental stages (Loh et al., 2004). This represents almost three times the number of claudin genes present in mammals. Furthermore, two distinct *tjp1/zo-1* and *tjp2/zo-2* genes each are present in fugu and zebrafish and expressed in a tissue and developmental stage specific manner in zebrafish (Kiener et al., 2007). In the present study we explored the functional role of *tjp3/zo-3* during zebrafish development. We show that *tjp3/zo-3* is a component of TJs found in the EVL of zebrafish embryos. Silencing *tjp3/zo-3* expression leads to a defective EVL barrier, resulting in an increased sensitivity of embryos to osmotic stress.

Materials and methods

Antibodies

Commercial antibodies used for immunohistochemistry or Western blot analysis and their source are listed in the description of the respective techniques below. A GST fusion protein containing the C-terminal part of the zebrafish Tjp3/Zo-3 was purified and used to immunize rabbits (BioGenes, Berlin, Germany). The antisera were affinity purified and used for immunoblotting and immunolabeling.

Zebrafish embryo culture

Care and breeding of zebrafish was carried out according to international and institutional standards. The AB wild-type (WT) zebrafish line from the in house stock was used. WT embryos were collected from multiple pair matings. All embryos were maintained in egg water at 28 °C. For experiments using embryos older than 6 hpf, 0.2 mM phenylthiourea was added to the egg water to prevent pigmentation and tricaine was used as an anesthetic before processing. Staging was done according to hours postfertilization (hpf) (Kimmel et al., 1995).

Zebrafish embryo microinjection

The following antisense morpholino oligonucleotides (MOs) were obtained from Gene Tools (Philomath, OR): a translation blocking morpholino 5′-GCTCCCATATCGTCATCTCCTCCAT-3′ (hybridizes to the start codon and the following 25 bases of *tjp3/zo-3* mRNA) and a splice inhibition morpholino 5′-ACCTCGCCACTTACTTTCGATAACG-3′ (hybridizes to bases 38 to 48 of the first exon and bases 1 to 14 of the first intron of the *tjp3/zo-3* transcript). Both MOs target the two putative *tjp3/zo-3* splice variants in zebrafish (Kiener et al., 2007). A standard control MO (5′-CCTCTTACCTCAGTTACAATTTATA-3′) with no target in zebrafish (www.gene-tools.com) was used as control. MO sequences were blasted against NCBI and Ensemble zebrafish genome assemblies and no significant similarities to other genomic loci besides zebrafish *tjp3/zo-3* were found. Zebrafish embryos were pressure injected at the 1-cell stage with 1.5 nl MO or expression vector, or both. *tjp3/zo-3* splice MO was injected at different concentrations (2 ng, 4 ng, 6 ng, 12 ng) and the phenotypes assessed by morphological criteria. A reproducible phenotype emerged with the injection of 6 ng *tjp3/zo-3* splice MO and this amount was used in subsequent experiments. The conventional translation blocking morpholino (ATGmo) was injected at 1 ng. As a negative control, the same amounts of the standard control morpholino were injected. For rescue experiments, 10 pg of pcDNA3.1 expression vector containing an N-terminal Flag tagged zebrafish or dog *TJP3/ZO-3* cDNA were injected alone or together with 6 ng of the *tjp3/zo-3* splice MO.

RT-PCR

Total RNA was isolated from zebrafish embryos using the RNeasy Mini kit (Qiagen). 1 mg of total RNA was amplified with the 1-step RT-PCR kit from Qiagen using gene-specific primers. Reverse transcription was performed at 50 °C for 30 min and amplifications with Taq polymerase were done using 35 cycles of denaturation (96 °C for 30 s), annealing (51 °C–57 °C for 30 s) and elongation (72 °C for 2 min). The following gene specific primers were used: *tjp3/zo-3* flanking the first intron; 5′-agaggcgaggtgttcagagtggtggac-3′ and 5′-aagatcaatgcgtgcagaaaacagagt-3′.

Immunoblotting

To isolate membrane-associated proteins, zebrafish embryos were homogenized in imidazole buffer (10 mM imidazole pH 7.4, 4 mM EDTA, 1 mM EGTA, 0.2 mM DTT, 100 mg/ml PMSF, 10 mg/ml CLAP) and centrifuged at 4 °C and 8000 rpm for 10 min. The pellet was resuspended in 6 M urea buffer (6 M urea, 10 mM Tris pH 8.0, 1 mM EDTA, 150 mM NaCl, 1 mM DTT, 100 mg/ml PMSF, 10 mg/ml CLAP), vortexed, and centrifuged at 4 °C and 13,000 rpm for 1 h. The protein concentration of the supernatant enriched in the membrane-associated proteins was determined using the Bradford assay (Pierce). Proteins were separated by SDS-PAGE using 10% polyacrylamide gels and transferred to PVDF membranes (Amersham). Membranes were incubated with affinity purified anti-Tjp3/Zo-3 (1:500 dilution) or M2 anti-Flag (Sigma; 1:1000 dilution) in PBS, 0.5% BSA, followed by HRP-conjugated secondary antibodies (BioRad; 1:3000 dilution), and processed for chemiluminescence detection (Supersignal West Pico, Pierce and Amersham films).

Immunolabeling

For immunofluorescence detection of proteins on whole mount embryos or cryosections, embryos were fixed in 4% PFA in PBS. For cryosectioning, embryos were embedded in 1% bacto-agar in PBS and cryoprotected by overnight saturation in 30% sucrose. 15 μm sections were cut using a Zeiss cryostat and collected on polylysine coated slides (Menzel-Glaesser, Germany). Affinity purified anti-Tjp3/Zo-3 (1:250), anti-ZO-1 (Zymed, 1:500), anti-Flag (Sigma, 1:1000), anti-β-catenin (Transduction Laboratories, 1:1000), anti-E-cadherin (Transduction Laboratories, 1:500), anti-PKCζ (Santa Cruz, 1:500) and anti-Na+/K+-ATPase (a6F, 1:100) antibodies were diluted in PBS, 10% NGS, 0.5% Triton-X100. Alexa-488 and/or Alexa-596 goat anti-rabbit or anti-mouse secondary antibodies (Molecular Probes) were diluted 1:1000. Images were acquired using an Axiocam camera on a Zeiss microscope.

In situ hybridization

Plasmids containing zebrafish *tjp3/zo-3* (pBluescript) and Pax2b (pScript) cDNAs were linearized and antisense mRNA was transcribed by T7 RNA polymerase (NEB) in the presence of dioxigenin-UTP (Roche). In situ hybridization of whole mount zebrafish was performed essentially as described (Hauptmann and Gerster, 1994).

Electron microscopy

Three control, three *tjp3/zo-3* ATGmo, and five *tjp3/zo-3* MO injected embryos were sectioned and stained for electron microscopy. For each embryo, two grids were examined for EVL cell contacts. All contacts between adjacent EVL cells were counted and classified into one of three groups depending on weather the electron dense plaque between adjacent EVL cells characteristic for TJ showed normal morphology, blebbing, or was absent. Numbers were subjected to *t*-test analysis to establish significant differences.

Biotin permeability assay

At 6 hpf, zebrafish embryos were dechorionized and exposed to 1 mg/ml S-NHS-Biotin (Pierce) in PBS for 30 min at 4 °C to prevent endocytosis. Embryos were then washed in PBS, 100 mM glycine and immediately fixed in 4% PFA for 1 hr at RT, embedded in agar and cryoprotected in 30% sucrose before sectioning. Sections were incubated with Alexa-488 labeled streptavidin, viewed under the microscope and digital photographs were acquired using the same settings and exposure times for each slide.

Osmotic sensitivity and cadmium toxicity assays

Embryos were dechorionized at 6 hpf and grown in either 1× egg water (0.9 mM/1.8 mosM red sea ocean salt), 20× egg water (18 mM/36 mosM ocean salt), 50× egg water (45 mM/90 mosM ocean salt); 100× egg water (90 mM/180 mosM ocean salt); 10× NaCl (157 mM/314 mosM NaCl in egg water); 20× $CaCl_2$ (43 mM/112 mosM $CaCl_2$ in egg water); or 20× $MgSO_4$ (37 mM/74 mosM $MgSO_4$ in egg water). The osmolarity of each solutions was less than the estimated physiological osmolarity of zebrafish (230–300 mosM), except for 10× NaCl (314 mosM). Mortality was assessed at 1 dpf. Experiments were done at least in triplicates and subjected to *t*-test analysis to establish statistical significance. To correlate the mortality to the *tjp3/zo-3* morphant phenotype, the number of surviving morphants was counted after 2 dpf and 2-way analysis of variance (ANOVA) was performed to establish statistical significance. To assess the sensitivity to cadmium, embryos were grown in 0.5 mM or 1 mM $CdCl_2$ in egg water from 8 hpf up to 2 dpf. Dead embryos were counted at 2 dpf. Again, experiments were done at least in triplicates and subjected to 2-way ANOVA to establish statistical significance.

Reversal of edema

At 2 dpf *tjp3/zo-3* morphants were transferred into a hyperosmotic 300 mM sucrose solution and the number of embryos with pericardial edema was determined at 3 dpf. Mortality was determined at 3 dpf and 4 dpf for both control and morphant embryos. Experiments were done at least in triplicates and subjected to *t*-tests to establish statistical significance.

Results

Tight junction formation and tjp3/zo-3 expression in early zebrafish embryos

Tjp3/zo-3 is a maternally supplied mRNA with a uniform expression from the 2-cell stage to the time of gastrulation as detected by in situ hybridization (Figs. 1A–D). Apical junctions are formed as early as the 8-cell stage, when an accumulation of Tjp1 could be detected at cell–cell contact sites (Fig. 1J). However, Tjp3/Zo-3 protein was incorporated into tight junctions only at the 64-cell stage, when it was first detected at cell–cell contact sites in the EVL (Fig. 1G). By the time of gastrulation, the EVL cells were all surrounded with tight

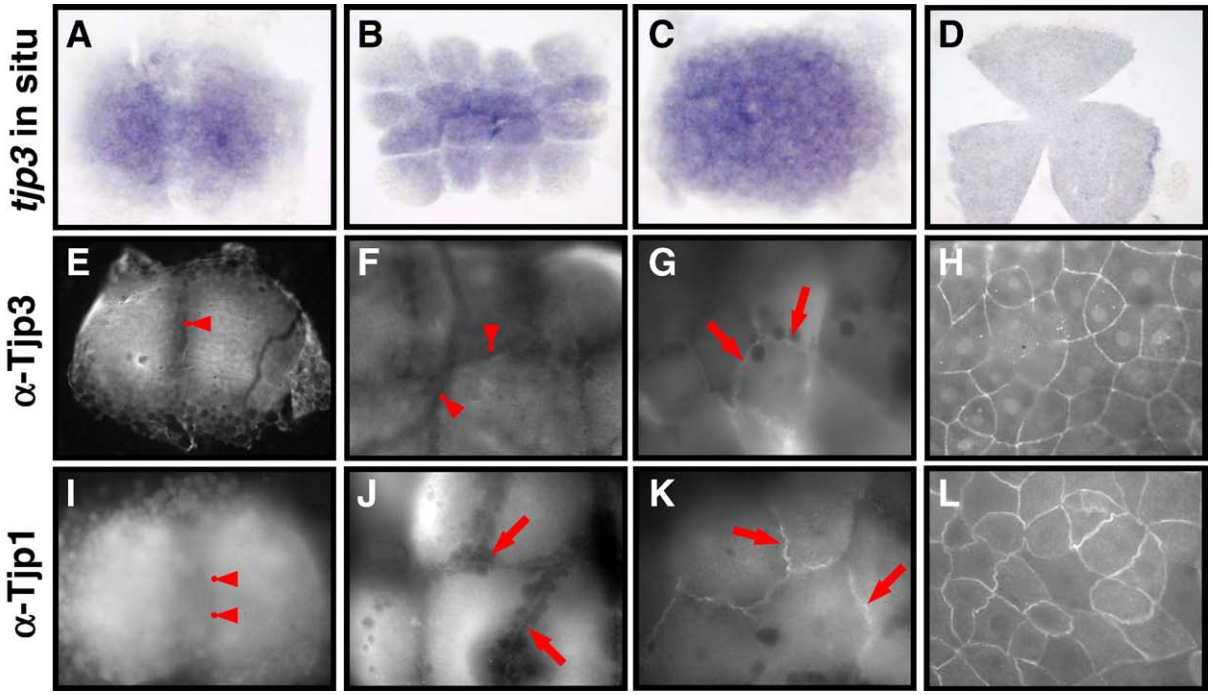

Fig. 1. Tight junction biogenesis in the early zebrafish embryo. *Tjp3/zo-3* whole mount in situ hybridization (A–D) and Tjp3/Zo-3 (E–H) and Tjp1/Zo-1 whole-mount immunofluorescence (I–L) of 2-cell stage/0.75 h (A, E, I); 8–16-cell stage/1.25 hpf (B, F, J); 64-cell stage/2 hpf (C, G, K); shield stage/6 hpf (D, H, L). *Tjp3/zo-3* is a maternally supplied mRNA with in situ hybridization signals from the 2-cell stage (A–C). Expression is uniform up to 60% epiboly (D). Tjp1/Zo-1 and Tjp3/Zo-3 are already present in the 2-cell stage embryo, where they are localized diffusely in the cytoplasm but not at cell–cell contact sites (E, anti-Tjp3/Zo-3; I, anti-Tjp1, arrowheads). Tjp3/Zo-3 remains absent from cell–cell contact sites at the 8-cell stage (F, arrowheads) but Tjp1/Zo-1 already accumulates at cell–cell junctions (J, arrows). Tjp3/Zo-3 gets localized to cell–cell contacts only at the 64-cell stage (G, arrows), by a time when Tjp1/Zo-1 is strongly present in the junctional complex (K, arrow). By 6 hpf the enveloping cell layer contains Tjp3/Zo-3 and Tjp1/Zo-1 at all cell–cell junctions (G, H).

junctions (Figs. 1H, L). During somitogenesis *tjp3/zo-3* hybridization signals become localized to the olfactory placodes, otic placodes, pronephric ducts and the epidermis. At the larval stage, *tjp3/zo-3* is strongly expressed in the pronephric ducts, intestine and stomach, while the epidermis maintains a low level of expression. In the anterior embryo, *tjp3/zo-3* gene is expressed in the nose, ears, branchial arches and midbrain (Kiener et al., 2007).

Repression of tjp3/zo-3 expression results in a specific morphant phenotype

In order to explore the role of Tjp3/Zo-3 in early development, *tjp3/zo-3* expression was knocked down using two different MOs. The first MO was a standard translation blocking morpholino (ATGmo) spanning the translation start site of the tjp3/zo-3 mRNA. The second was a splice inhibition morpholino (MO) against the first exon/intron boundary of the zebrafish *tjp3/zo-3* gene, inhibiting splicing and leading to the translation of the first exon and part of the first intron up to an in frame stop codon. As a result, a truncated Tjp3/Zo-3 protein containing only the first 16 N-terminal amino acids and no functional protein domains was translated. Inhibition of splicing was monitored by RT-PCR using primers flanking the first intron, resulting in a longer PCR fragment (210 bp) when compared to properly spliced wild-type mRNA (97 bp) (see below). A standard control morpholino (Cmo) without known target in zebrafish served as a control. Zebrafish embryos were injected at the 1-cell stage with *tjp3/zo-3* MO, *tjp3/zo-3* ATGmo or Cmo, and analyzed by live imaging, RT-PCR, Western blot, and immunolabeling.

Embryos injected with either the *tjp3/zo-3* MO or ATGmo presented essentially the same phenotypes. At 1 dpf, morphant embryos had shorter and curved tails with an expanded blood island (Fig. 2A). Several fish showed an overall reduction in body length and first signs of pericardial edema. By 2 dpf, pericardial edema was pronounced and many fish lacked blood circulation. Morphants had curved tails and the size of the tailfin was reduced (Fig. 2A). No phenotypes were observed for Cmo injected embryos.

To confirm the activity of the MOs, RT-PCR analysis was performed on embryos injected with either *tjp3/zo-3* MO or Cmo. In Cmo injected embryos, primers flanking the first exon amplified a single fragment of 97 bp, indicating proper splicing of exon 1 and 2 (Fig. 2B). In embryos injected with *tjp3/zo-3* MO and selected for the absence of a phenotype, an additional 210 bp fragment was amplified. The longer fragment contained sequence from the first intron, indicating that the MO interfered with the proper splicing of exon 1 and exon 2. The 210 bp fragment was predominantly amplified from MO injected zebrafish selected for the presence of a phenotype.

Western blot analysis and immunolabeling confirmed the loss of Tjp3/Zo-3 in morphants. Protein extracts from 6 hpf embryos showed a loss of Tjp3/Zo-3 even before any phenotype could be observed (Fig. 2C, lanes 1–3). Abundant Tjp3/Zo-3 protein was detected by Western blots in extracts from 2 dpf embryos injected with Cmo, whereas little if any was present in *tjp3/zo-3* MO or ATGmo injected embryos presenting a phenotype. The loss of Tjp3/Zo-3 correlates to the morphant phenotype as MO injected embryos without apparent phenotype retained Tjp3/Zo-3 (Fig. 2C, lanes 4–7). Furthermore, Tjp3/Zo-3 protein detected by immunolabeling in the olfactory placodes, otic placodes, epidermis, pronephric ducts, and intestine of normal or Cmo injected embryos between 1 dpf and 6 dpf, was lost from morphants (Fig. 3). As observed above, the morphant phenotype correlated with the loss of Tjp3/Zo-3 as morpholino injected embryos selected for the absence of an apparent phenotype still expressed Tjp3/Zo-3 protein in these structures (data not shown).

Characterization of morphant phenotypes

To further explore the specificity of the morpholino induced phenotypes, the *tjp3/zo-3* morpholinos were injected at different concentrations and the phenotypes assessed based on morphological criteria. Injection of MO and ATGmo both caused the same distribution of phenotypes. The severity of the phenotypes was dosage dependent, but a 10 fold lower concentration of ATGmo was sufficient to induce the same phenotypes as compared to MO. This suggests that blocking ribosome attachment rather than splice site recognition is more efficient in inhibiting translation.

To characterize the different phenotypes, zebrafish embryos were injected at the 1-cell stage with 6 ng Cmo, 1 ng *tjp3/zo-3* ATGmo, or 2 ng, 6 ng or 12 ng *tjp3/zo-3* MO. Embryonic development was observed at different time points and phenotypes were classified and counted at the onset of gastrulation (shield stage, 6 hpf), during gastrulation (12 hpf), at the end of somitogenesis (1 dpf), and after organogenesis (2 dpf) (Fig. 4A).

At the shield stage, all injections resulted in ~15% deaths and <5% dumbbell-shaped embryos. These effects were also observed for Cmo injected embryos and considered the result of the injection procedure. The earliest defects could bee seen during somitogenesis (12 hpf) in a small number (<10%) of embryos that were slightly elongated with the tailbud pointing away from the yolk instead of growing towards the vegetal pole. The axis of these embryos was wider than that of WT embryos (data not shown).

At 1 dpf, the mortality rate was ~20% for Cmo and 2 ng or 6 ng MO injected embryos, but ~30% for 12 ng MO and 1 ng ATGmo injected embryos. Of the survivors ~15% (2 ng) to ~70% (12 ng) had tail malformations, predominantly a curved tail and/or smaller tail fin. In severe cases, the tail was bent at a 45° angle, posterior to the yolk extension ("curved tail" phenotype). The milder form ("small tailfin" phenotype) presented with a tail fin of only approximately half the normal width of WT embryos (Table 1). After 2 days of development, mortality levels further increased in the 6 ng and 12 ng MO groups to ~30% and ~40%, respectively. Of the survivors, ~40% (2 ng MO) to ~80% (12 ng MO) had circulation defects and/or tail malformations (Table 1; Fig. 4A).

The phenotypes were classified into four groups (I–IV) according to severity. Group I had no circulation with edema

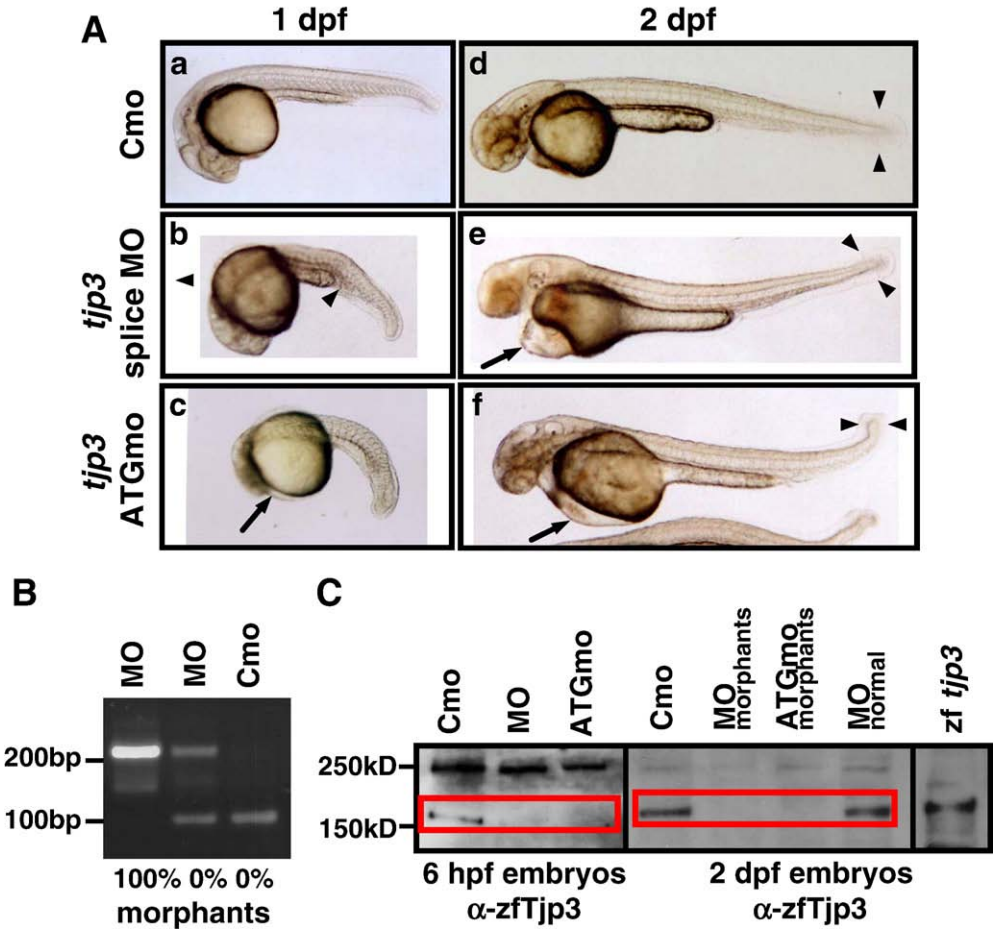

Fig. 2. Characterization of the *tjp3/zo-3* morpholino phenotype. Zebrafish embryos were injected with a control morpholino (Cmo), a splice site (MO) or a translation start morpholino (ATGmo) against *tjp3/zo-3*. (A) Both *tjp3/zo-3* splice and translation start morpholino injected embryos present the same phenotypes. At 1 dpf embryos had shorter and curved tails with an expanded blood island (b, arrowhead). Some individuals showed an overall reduction in body length and the beginning of pericardial edema (c, arrow). By 2 dpf, pericardial edema was pronounced (e, f, arrows) and many individuals had no blood circulation. Morphants had curved tails and the size of the tailfin was reduced (e, f, arrowheads). (B) *tjp3/zo-3* splice morpholino inhibits *tjp3/zo-3* mRNA splicing. RT-PCR analysis was performed on embryos injected either with control morpholino (Cmo), or *tjp3/zo-3* splice morpholino (MO) at 1 dpf. In control morpholino injected embryos, only one product of 97 bp corresponding to the properly spliced exon1/2 sequence was amplified (lane 3). In embryos injected with *tjp3/zo-3* splice morpholino and selected for normal phenotypes, a 210 bp fragment containing the first intron sequence was amplified in addition to the 97 bp WT fragment (lane 2). Abnormal phenotypes were characterized by the absence of the 97 bp WT fragment and the presence of the 210 bp exon1/intron1/exon2 fragment (lane 1). (C) The *tjp3/zo-3* splice and translation blocking morpholino reduce Tjp3/Zo-3 protein levels. Protein from whole 6 hpf (lanes 1–3) or 2 dpf (lanes 4–8) embryos was extracted and blotted with anti-zebrafish Tjp3/Zo-3 antibody. At 6 hpf, low levels of Tjp3/Zo-3 protein were detected in embryos injected with a control morpholino (Cmo, lane 1). No Tjp3/Zo-3 protein could be detected in embryos injected with *tjp3/zo-3* splice morpholino (MO, lane 2) or *tjp3/zo-3* translation blocking morpholino (ATGmo, lane 3). At 2 dpf both splice morpholino and ATG morpholino injected embryos were selected for morphant phenotypes. These individuals showed a strong reduction of Tjp3/Zo-3 protein levels (lanes 5 and 6) while splice morpholino injected embryos without phenotype had normal levels of Tjp3/Zo-3 protein (lane 7). WT embryos injected with Tjp3/Zo-3 expression vector served as a positive control (lane 8).

and a curved tail, category II edema with or without curved tail, group III a curved tail only, and class IV a smaller tailfin only. At high doses for both *tjp3/zo-3* morpholinos the major phenotype of the survivors was absent circulation with edema and a curved tail (2-way ANOVA, $p<0.01$), at low doses a smaller tailfin (Fig. 4B). Less than 3% cases of edema were observed at low doses. Pericardial edema was reversible and embryos of phenotype categories II, III and IV could be grown to adulthood. A reproducible distribution of phenotypes was observed with 1 ng of the translation blocking morpholino and 6 ng of the *tjp3/zo-3* splice morpholino and these amounts were used in subsequent experiments.

The morphant phenotype can be rescued by zebrafish tjp3/zo-3

If the phenotypes described above arise from a loss of *tjp3/zo-3*, they should be rescued by the *tjp3/zo-3* cDNA. 6 ng *tjp3/zo-3* splice morpholino was co-injected with 10 pg pcDNA3.1 expression vector containing either a Flag-tagged zebrafish *tjp3/zo-3* cDNA or a truncated form lacking the C-terminal Thr–Glu–Leu PDZ binding motif, or a Flag-tagged dog *TJP3/ZO-3* cDNA. At 1 dpf, embryos were classified as dead if they consisted of a mass of apoptotic tissue or morphants if they presented curved tails and an expanded blood island (see Fig. 2A). Embryos that had been co-injected with *tjp3/zo-3*

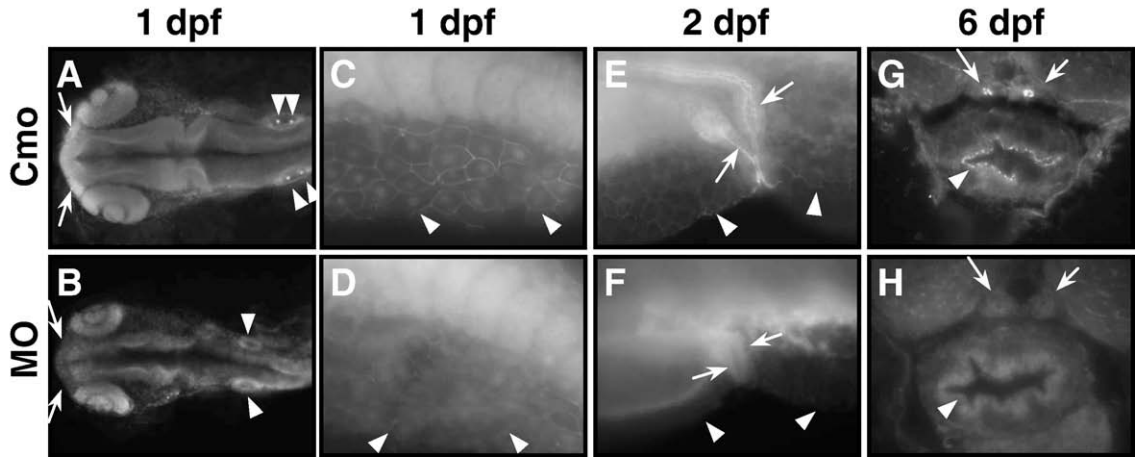

Fig. 3. The *tjp3*/*zo-3* morpholino causes the loss of Tjp3/Zo-3 protein expression. Immunofluorescence of whole mount zebrafish at 1 dpf (A–D), 2 dpf (E–F), and cryosections at 6 dpf (G–H) stained with anti-Tjp3/Zo-3. Tjp3/Zo-3 protein is lost in morpholino-injected embryos from 1 dpf up to 6 dpf. The morphant phenotype correlates to the loss of Tjp3/Zo-3 since embryos selected for the lack of an apparent phenotype still express Tjp3/Zo-3 protein (data not shown). At 1 dpf there is a loss of Tjp3/Zo-3 labeling in the olfactory placodes (A, B, arrows), otic placodes (A, B arrowheads), and skin (C–F arrowheads). At later stages, Tjp3/Zo-3 protein is absent from the apical membranes of the pronephric ducts (E–H, arrows), and intestine (G, H, arrowheads).

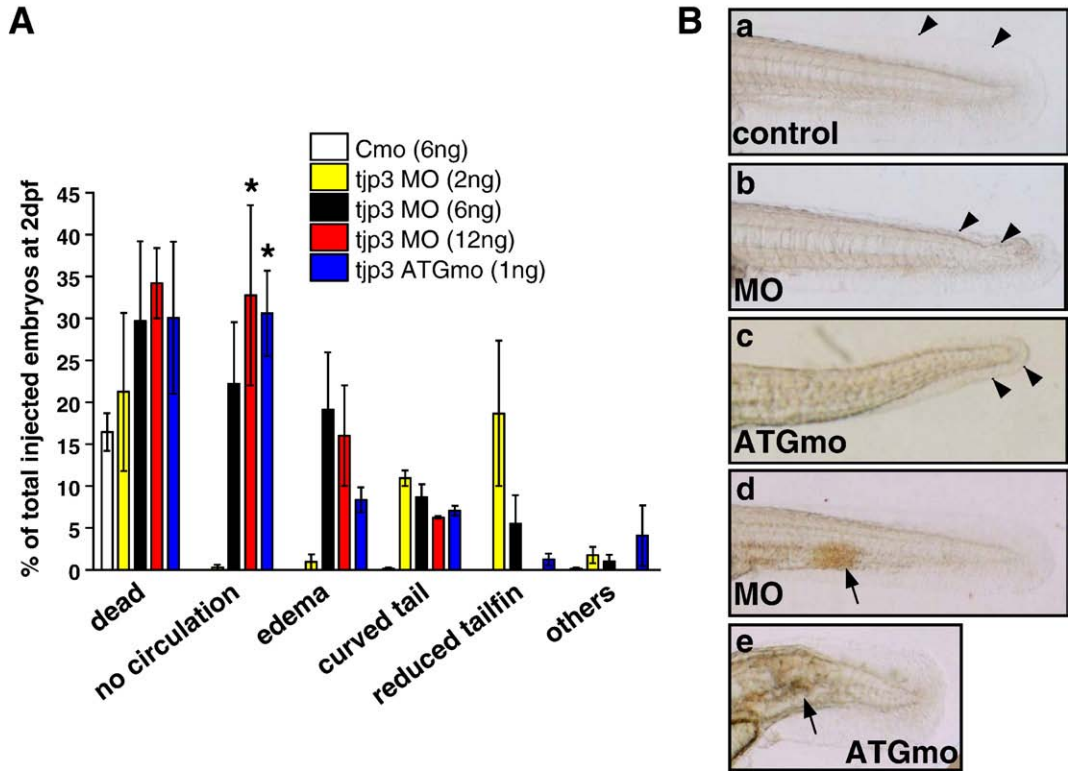

Fig. 4. The *tjp3*/*zo-3* morpholino effect is specific. Analysis of *tjp3*/*zo-3* morpholino injected embryos at 2 dpf showed that the severity of the phenotype is dosage dependent and that the injection of splice-site morpholino and translation morpholino cause the same distribution of phenotypes. (A) Zebrafish embryos were injected at the 1-cell stage with 6 ng/1.5 nl control morpholino, 1.5 nl *tjp3*/*zo-3* splice morpholino (MO) at different concentrations (2 ng, 6 ng, 12 ng) and 1 ng/1.5 nl *tjp3*/*zo-3* translation blocking morpholino (ATGmo). At 2 dpf the phenotypes were assessed by morphological criteria. The death rate was between 20% (2 ng MO) and 40% (12 ng MO). The phenotypes were classified into 4 groups according to severity: no circulation (with edema and curved tail), edema (with or without curved tail), curved tail only, and reduced tailfin only. At a high dose of *tjp3*/*zo-3* morpholino (12 ng) the major phenotype of the survivors was absent circulation with edema and a curved tail (55%), whereas at a low dose (2 ng) it was a reduction of the tailfin (20%) with less than 3% of edema. The injection of only 1 ng of translation blocking morpholino (ATGmo) resulted in a similar distribution of phenotypes as that of 12 ng splice morpholino (MO). Mean and S.E.M.; $n \geq 100$ per experiment; 3–5 independent experiments. 2-way ANOVA; $p < 0.05$ (12 ng MO), $p < 0.01$ (1 ng ATGmo). Asterisks indicate statistical significance. (B) Phenotypes of injected embryos at 2 dpf. Control morpholino injected embryo (a); *tjp3*/*zo-3* splice morpholino injected embryos (b, d); *tjp3*/*zo-3* translation blocking morpholino injected embryos (c, e). Mild phenotypes presented with crooked tail buds and reduced tailfin size (b, c, arrowheads), while severely affected embryos had no circulation and often an accumulation of red blood cells (d, e, arrows).

splice morpholino and *tjp3/zo-3* cDNA and had no apparent phenotypes were considered "rescued". Approximately 10% wild-type embryos injected with the Flag-tagged zebrafish but not the dog cDNA for *tjp3/zo-3* presented with a dramatically shortened, upwards curved body axis and apoptosis in the brain by 1 dpf, likely due to overexpression of the protein.

Co-injection of *tjp3/zo-3* splice morpholino and the full-length or truncated Flag-tagged zebrafish *tjp3/zo-3* cDNA lead to a significant reduction in the number of morphants (2-way ANOVA, $p<0.01$) with a corresponding increase in the number of apparently normal embryos, showing that the morpholino induced phenotype can be rescued. Interestingly, however, the phenotype could not be rescued by co-injection of the dog Flag-tagged *TJP3/ZO-3* cDNA (Fig. 5A). Fractionation of zebrafish embryo homogenates into cytosol and membrane fractions showed that the bulk of the dog *TJP3/ZO-3* was present in the

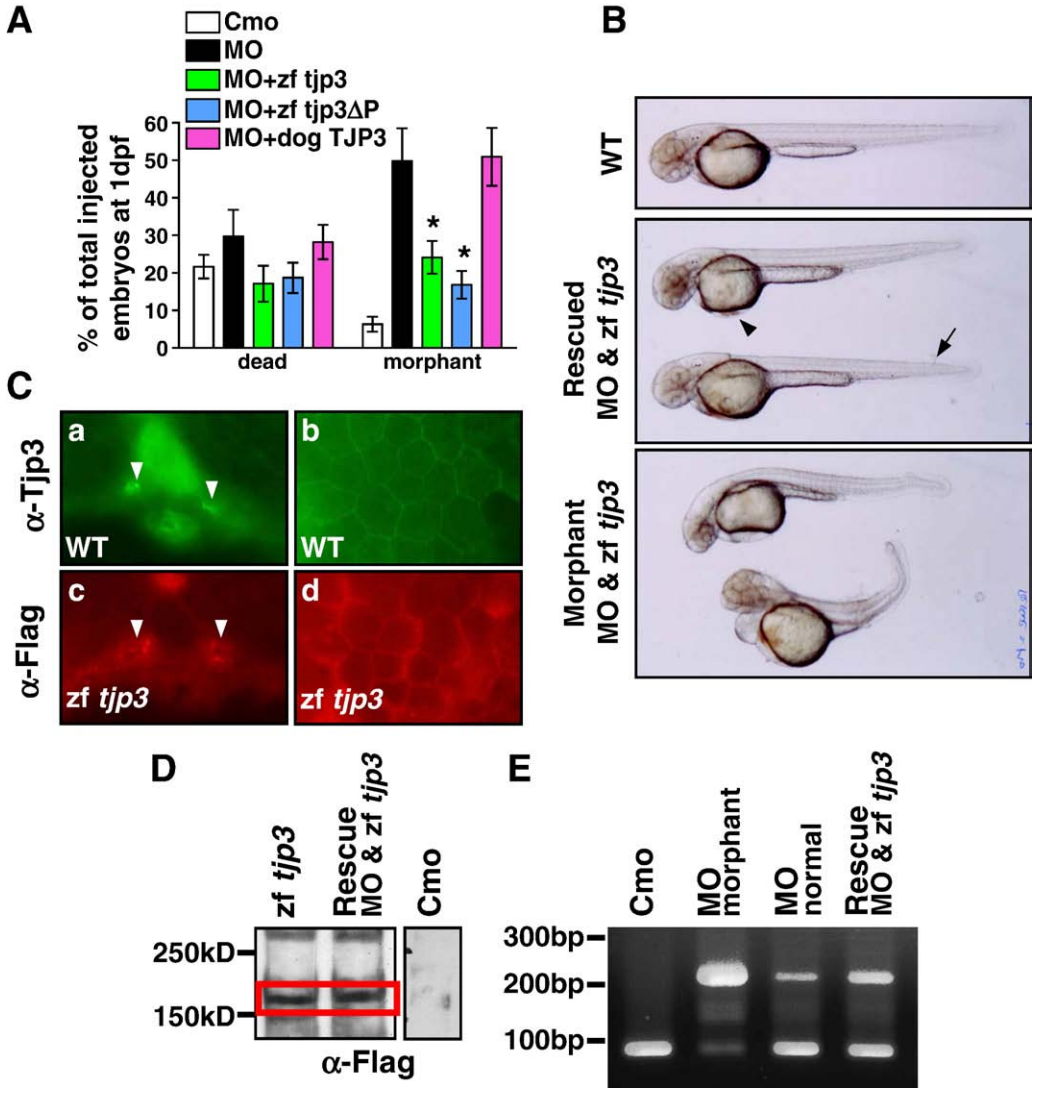

Fig. 5. Rescue of the phenotype. *Tjp3/zo-3* morphants can be rescued by full-length zebrafish *tjp3/zo-3* and a truncated zebrafish *tjp3/zo-3* without the C-terminal PDZ-binding motive, but not dog TJP3/ZO-3. (A) *tjp3/zo-3* morphants can be rescued by co-injection of *tjp3/zo-3* splice morpholino and pcDNA3.1 expression vector containing full-length Flag-tagged zebrafish *tjp3/zo-3* (zf *tjp3*) or mutant zebrafish *tjp3/zo-3* without the PDZ-binding motif (zf *tjp3*ΔP). Co-injection of pcDNA3.1 dog TJP3/ZO-3 cannot rescue the morphant phenotype, even tough the protein is expressed and enriched in membrane associated protein fractions of zebrafish (data not shown). Phenotypes were counted at 1 dpf. Mean and S.E.M.; $n \geq 100$ per experiment; 2–6 independent experiments. 2-way ANOVA; $p<0.01$. Asterisks indicate statistical significance. (B) Rescued embryos showed a straight body axis, little (arrowhead) or no edema, and only mild tailfin malformations (arrow). Non-rescued embryos presented with the morphant phenotype as described in Figs. 2 and 4. (C) Immunofluorescence on cryosections of WT embryos (a, b) and embryos injected with pcDNA3.1 Flag-tagged zebrafish *tjp3/zo-3* (c, d) at 2 dpf. WT embryos were labeled with Tjp3/Zo-3 antibody to detect endogenous Tjp3/Zo-3 localization (a, b). Ectopically expressed Tjp3/Zo-3 localizes accurately. Anti-Flag staining was detected in the apical side of the pronephric ducts (c, arrowheads) and in the skin (d). (D) Anti-Flag Western blot at 2 dpf. Embryos were injected with control morpholino (Cmo), pcDNA3.1 zebrafish *tjp3/zo-3* (zf *tjp3*), or co-injected with morpholino and pcDNA3.1 zebrafish *tjp3/zo-3* (rescue). Ectopic Flag-tagged Tjp3/Zo-3 is expressed in embryos injected with tjp3/zo-3 alone (lane 1) as well as in the rescued embryos (lane 2). No Flag labeling was detected in controls (lane 3, different experiment). (E) RT-PCR analysis was performed using total RNA of 2 dpf embryos to check for the activity of the splice morpholino in rescued embryos. In control embryos (lane 1) and in morpholino injected embryos without phenotypes (lane 3), the properly spliced 97 bp wt band was amplified predominantly. However, *tjp3/zo-3* morphants had a strong unspliced band at 210 bp (lane 2), which was also present in rescued embryos (lane 4).

membrane-associated fraction (data not shown), consistent with its incorporation into TJs.

Rescued embryos were nearly identical to wt embryos. They had a straight body axis, little or no edema, and only occasionally could we observe slight tailfin malformations. The 15% to 20% of non-rescued embryos presented the classical morphant phenotype with a shorter and/or curved body axis, severe pericardial edema and pronounced tailfin malformations as described above (Fig. 5B).

Immunolabeling with Flag antibodies confirmed that injection of pcDNA3.1 vector leads to the expression of ectopic zebrafish Tjp3/Zo-3. Flag-tagged protein accurately localized to the lumenal pole of epithelial cells of the pronephric ducts, as well as to the skin (Fig. 5C).

To confirm expression of the ectopic zebrafish Tjp3/Zo-3 in rescued embryos, protein was extracted from 2 dpf embryos and blotted with anti-Flag antibody. Flag-tagged zebrafish Tjp3/Zo-3 was detected in both embryos injected with zebrafish *tjp3/zo-3* alone as well as in rescued embryos where zebrafish *tjp3/zo-3* was co-injected with the *tjp3/zo-3* morpholino (Fig. 5D, lanes 1–2). No Flag labeling was observed in control embryos (Fig. 5D, lane 3).

Since not all *tjp3/zo-3* MO injected embryos displayed a phenotype, it was important to confirm that the splice morpholino was indeed active in the rescued embryos. In Cmo injected embryos and in MO injected embryos selected for the absence of phenotypes, the properly spliced 97 bp WT RT-PCR fragment was predominantly amplified from 2-dpf embryo RNA (Fig. 5E). *Tjp3/zo-3* morphants showed a prominent 210 bp fragment, indicative of failed splicing due to the action of the morpholino. Importantly, the 210 bp fragment was also present in rescued embryos. The slightly lower levels of the 210 bp compared to the 97 bp fragment in the rescued embryos most likely reflects the presence of a small fraction of indistinguishable "normal" embryos where the splice morpholino was inactive. Thus, zebrafish Tjp3/Zo-3 can rescue the morpholino-induced phenotypes.

Tight junction structure in the EVL of tjp3/zo-3 morphants is altered

In the early zebrafish embryo, the EVL, a specialized layer of flat and elongated cells, forms a primary "skin", which serves as a barrier between the embryo proper and the surrounding fresh water environment (Kimmel et al., 1990). Given the function of the EVL as a barrier and the incorporation of Tjp3/Zo-3 into TJs as early as the 64-cell stage (see Fig. 1G), we speculated that the EVL may establish TJs and that these may be affected by the loss of Tjp3/Zo-3 in the morphants, leading to some of the phenotypes described above.

Immunolabeling of embryos at the onset of gastrulation (6 hpf) showed a concentration of Tjp3/Zo-3 and Tjp1/Zo-1 at sites of cell–cell contact facing the external environment (Fig. 6A). At least by real-time RT-PCR, no significant changes in the expression levels for the other Tjps were observed. Analysis of embryo sections by transmission electron microscopy (TEM) confirmed the presence of electron dense regions where the intercellular space between the lateral membranes of adjoining cells was obliterated, a characteristic feature for TJs (Fig. 6B). In ~40% of morpholino injected embryos, the Tjp3/Zo-3 protein was lost from the majority of the cell–cell contact sites in the EVL (Fig. 6A, b) whereas Tjp1 could still be detected at these sites (Fig. 6A, d).

To determine if the *tjp3/zo-3* morpholino affected the architecture of TJs, morphant embryos were analyzed by TEM. Cell–cell contacts between EVL were analyzed for the presence of TJs and these were classified into three groups based on their morphology. The first group included apparently normal TJs with the plasma membrane of neighboring EVL cells in close contact throughout the length of the adhesion plaque. A second class represented TJs with discontinuities in the adjoining plasma membranes, resulting in blebs. The third group represented the complete loss of the characteristic electron dense plaque.

In control embryos, TJs were readily detected at all contact sites between EVL cells (Fig. 6B, arrow) and only ~20% of TJs showed discontinuities. Splice morpholino injected embryos retained TJs between ~60% of EVL cells, but more than 40% of these TJs showed blebbing (Fig. 6B, red arrows). The remaining contact sites lacked electron dense plaques (Fig. 6B, arrowheads). When embryos were injected with ATGmo, as many as 60% of EVL cell–cell contact sites did not have a visible TJ plaque (Fig. 6B, arrowheads). Quantification of these results is shown in Fig. 6C. There was a significant reduction of normal electron dense TJ plaques in both MO and ATGmo injected embryos (*t*-tests, $p<0.05$). These findings confirm a defect in the morphology of TJs in the EVL cell layer of *tjp3/zo-3* morphants.

As injection of both splice and ATG morpholino resulted in the same phenotypes, e.g. the loss of the protein already at 6 hpf and the disrupted TJ ultrastructure, only the data for the splice morpholino is shown for subsequent experiments.

The asymmetric distribution of plasma membrane proteins is unaffected in tjp3/zo-3 morphants

TJs have been implicated in maintaining the asymmetric distribution of proteins to the apical and basolateral plasma membrane domains of epithelial cells (i.e. "fence function"). We therefore analyzed the polarized distribution of several markers in the EVL at 6 hpf. Since *tjp3/zo-3* is also highly expressed in the pronephric ducts (Kiener et al., 2007), the distribution of apical and lateral proteins in renal epithelial cells was also analyzed at 2 dpf. E-cadherin and β-catenin, two markers of adherens junctions, remained restricted to the lateral domain of the cells of the EVL of morpholino-injected embryos (Fig. 7A). Similarly, despite the loss of Tjp3/Zo-3 in the pronephric ducts of the morphants (Fig. 7B, d), E-cadherin and Na+/K+-ATPase retained their basolateral distribution (Figs. 7B, d and B, f) and atypical PKCζ remained localized to the apical domain (Fig. 7B, f). Whole mount in situ hybridization to detect expression of the early kidney marker *pax2b* showed a normal development of the pronephric ducts in morphants (Fig. 7BA, a, b), indicating

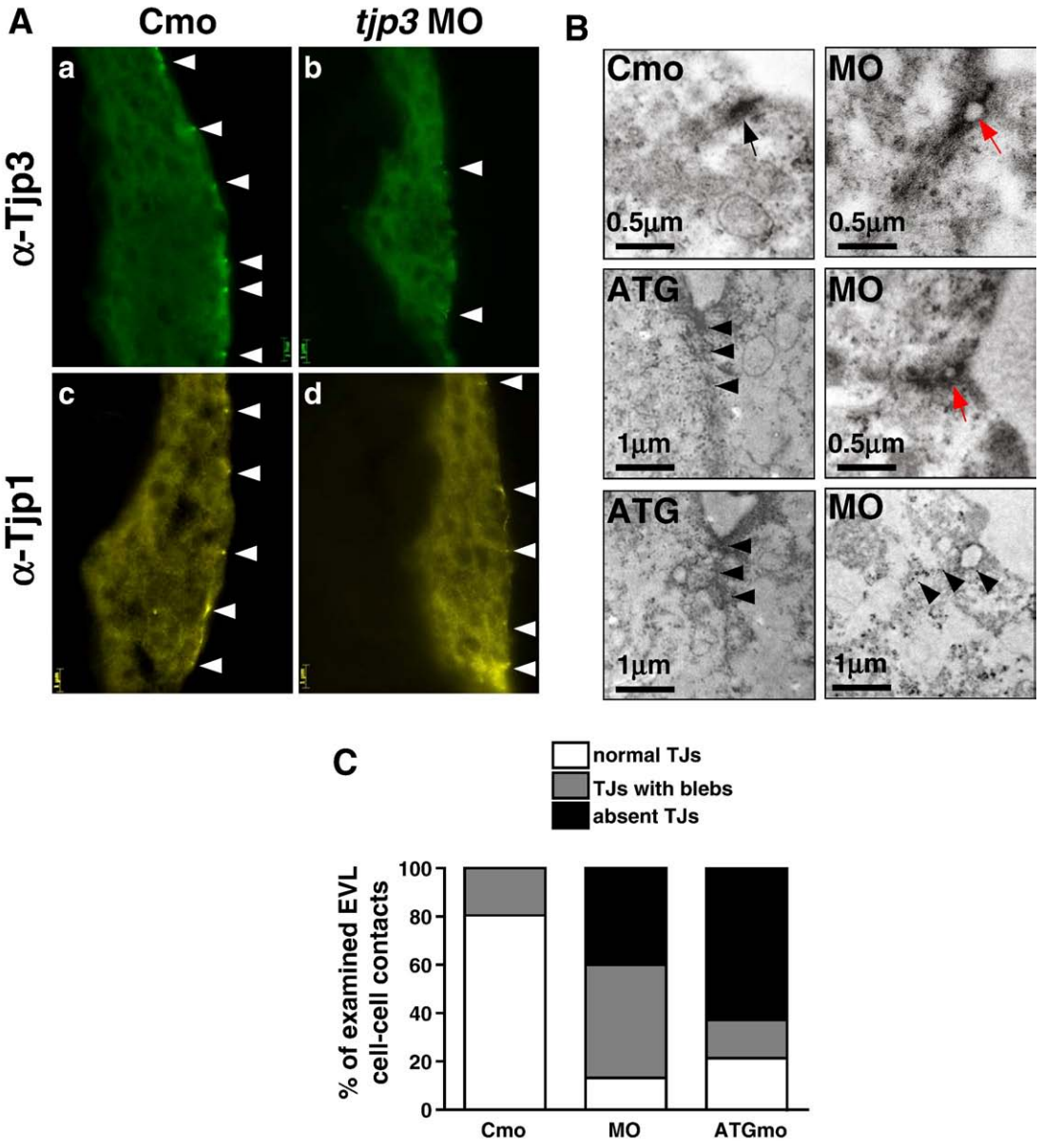

Fig. 6. The loss of Tjp3/Zo-3 leads to a disruption of the TJ ultrastructure. (A) Cryosections of 6 hpf embryos stained with anti-Tjp3/Zo-3 (a, b) and anti-Tjp1/Zo-1 (c, d). Embryos were injected with control morpholino (a, c, Cmo) or *tjp3/zo-3* splice morpholino (b, d, MO). Tjp3/Zo-3 protein is absent from most TJs in the EVL of morpholino injected embryos (b), but no phenotype is observed at that stage yet. The same embryos show a slight reduction in Tjp1/Zo-1 staining (d). (B) TEM of morpholino injected embryo sections show a marked loss and/or a disruption of the electron dense plaque of junctions in the EVL of morphants at 6 hpf. In control morpholino injected embryos, TJs can be observed at every cell–cell contact between neighboring cells of the EVL (Cmo, arrow). In the splice morpholino injected embryos, more than 40% of the EVL cell–cell contacts had discontinuities (blebbing) (MO, red arrows) and another 40% of contacts did not have any electron dense plaque (MO, arrowheads). Embryos injected with *tjp3/zo-3* translation blocking morpholino had an even greater number of missing TJs (ATG, arrowheads). (C) Statistical analysis of TJ integrity as seen in TEM at 6 hpf. Two control and five morpholino injected embryos were analyzed. All contacts between adjacent EVL cells were classified into one of three groups. 1) Normal TJs, where cell membranes were in close contact throughout the length of the TJ, 2) discontinuous TJs with blebs, where cell membranes detached from each other, thus reducing the effective length of the TJ seal, and 3) junctions where no electron dense plaque was found between neighboring EVL cells. About 25% of TJs in control embryos had blebs (bar 1). In splice morpholino injected embryos, 47% of TJs showed blebbing and another 40% of the junctions were missing an electron dense plaque (bar 2). 62% of EVL cell–cell contacts in ATGmo injected embryos lacked an electron dense plaque (bar 3). $N=3$ for Cmo, $n=3$ for ATGmo, $n=5$ for splice MO; number of cell–cell contacts counted per embryo 6–9; 2 independent experiments; *t*-test; $p<0.05$.

that Tjp3/Zo-3 is not critical for renal development. Similar findings were made for 1 dpf embryos and for ATGmo injected embryos (Supplemental Data I). Thus, epithelial cell polarity in the EVL and the pronephric ducts is not affected in *tjp3/zo-3* morphants.

Tjp3/Zo-3 is required for epidermal barrier function

We next determined weather a second function of TJs, the establishment of paracellular diffusion barriers, was affected in the EVL of *tjp3/zo-3* morphant embryos.

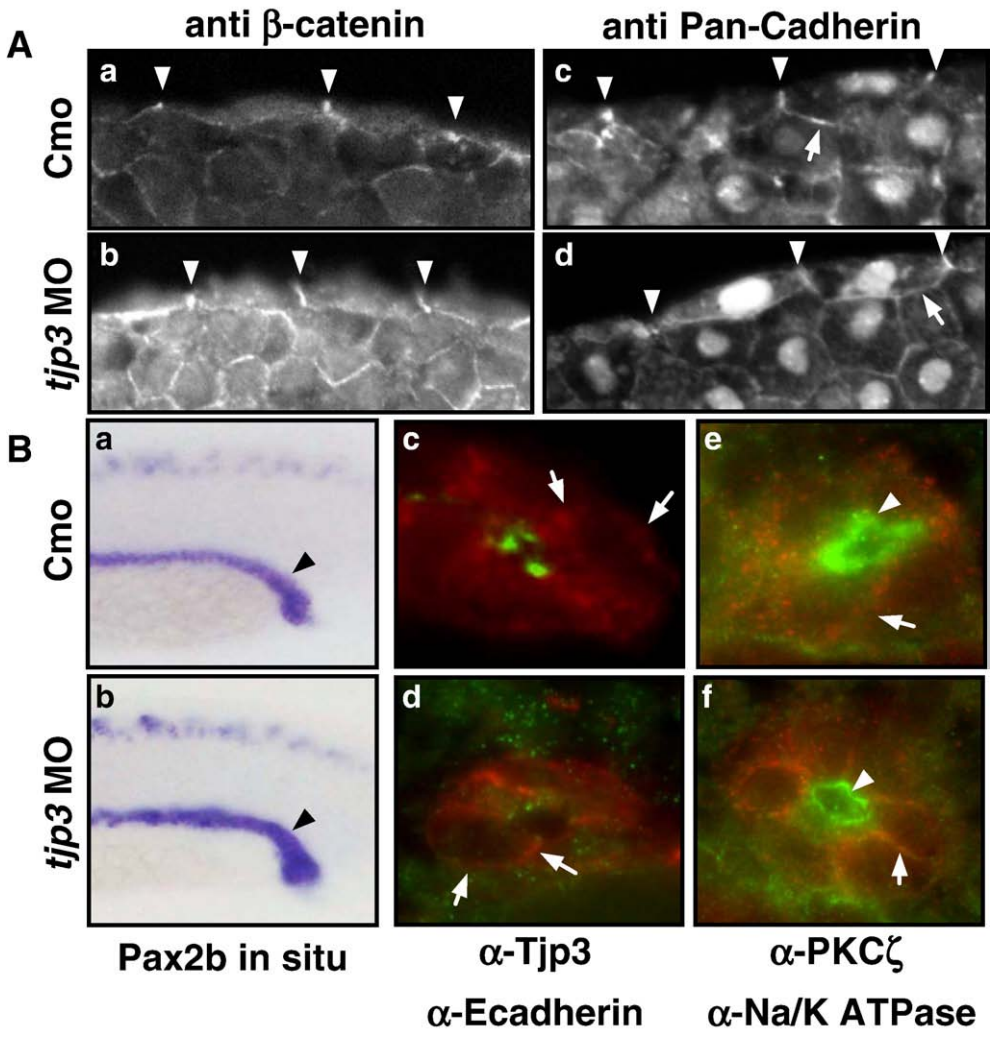

Fig. 7. The asymmetric distribution of plasma membrane proteins is maintained in *tjp3/zo-3* morphants. (A) Epithelial cell polarization in the EVL. Cryosections of control morpholino (a, c) and *tjp3/zo-3* morpholino (b, d) injected embryos at 6 hpf. The EVL, a monolayer of epithelial cells that surrounds the blastoderm, is shown. EVL cells retain their elongated, flattened morphology in the morphants (b, d). These cells are still polarized with adherens junctions along their basolateral membranes, as shown by labeling with anti β-catenin (a, b) and anti pan-Cadherin (c, d) antibodies. Both markers remained restricted to the basolateral surfaces (lateral membranes, arrowheads; basal membranes, arrows). (B) Epithelial cell polarization in the pronephric ducts. Whole mount in situ hybridization of Pax2b (a, b); Immunofluorescence on cryosections: anti-Tjp3/Zo-3 (green) and anti-E-cadherin (red) (c, d); anti-PKCζ (green) and anti-Na^+/K^+-ATPase (red) (e, f). Control morpholino 1 dpf (a, c, e); *tjp3/zo-3* morpholino 1 dpf (b, d, f). In situ hybridization with Pax2b shows that the pronephric ducts extend normally in *tjp3/zo-3* morphants (a, b, arrowheads). Morphants lost Tjp3/Zo-3 protein from the apical side of the pronephric ducts as shown above (c, d). E-cadherin staining of the basolateral membranes of the pronephric ducts is maintained in morphants (d, arrows). The polarized distribution of the basolateral Na^+/K^+-ATPase (e, f, arrows) and the apical PKCζ (e f, arrowheads) are also maintained in the pronephric duct.

First, we analyzed the diffusion of sulfo-NHS-biotin, a small (MW ~ 440 Da) membrane impermeable tracer often used to assess the intactness of the TJ barrier (Fesenko et al., 2000; Furuse et al., 2002; Merzdorf et al., 1998). Control morpholino or *tjp3/zo-3* morpholino injected embryos were dechorionized at 6 hpf and exposed to sulfo-NHS-biotin for 30 min. Following fixation, the biotin was detected in embryo sections using labeled streptavidin. In controls, only a weak staining in the EVL cell layer and the underlying blastoderm was observed (Fig. 8A). In contrast, however, a striking accumulation of biotin in the segmental cavity between the blastoderm and YSL was found in morphants. Of the morpholino injected embryos, ~50% showed increased biotin permeability, hence correlating with the observed penetration rate of 40–60% for the phenotype based on morphological assessment. A similar increased accumulation of biotin was observed in ATGmo injected embryos (Supplemental Data II).

To further corroborate the increased biotin permeability in morphant embryos, we next determined if these embryos were more sensitive to the toxicity of $CdCl_2$. Embryos were grown to 2 dpf in egg water supplemented with $CdCl_2$ at a concentration of low (0.5 mM) or high (1 mM) toxicity (Konishi et al., 2006) and mortality rates were determined. A significant increase in the mortality rate of control embryos was only observed in the presence of 1 mM $CdCl_2$, but not at the lower concentration (Fig. 8B). In contrast, the mortality rate of *tjp3/zo-3* morphants was already significantly higher at 0.5 mM $CdCl_2$ as compared to untreated morphants (Fig. 8B; 2-way ANOVA, $p < 0.01$). An

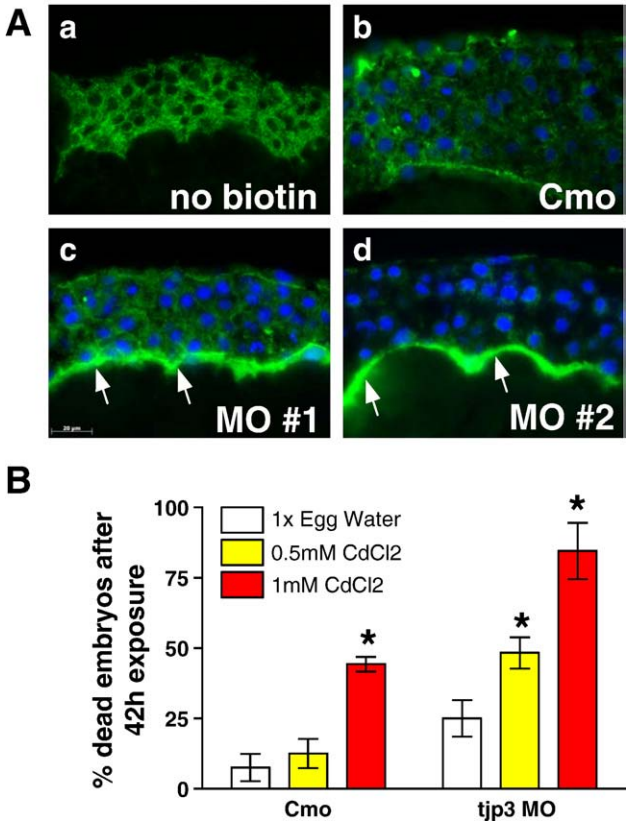

Fig. 8. Tjp3/Zo-3 is essential for EVL permeability barrier function. (A) Biotin permeability assay: negative control without biotin (a), control morpholino (b) and *tjp3/zo-3* morpholino (c, d) injected embryos were dechorionized at 6 hpf and exposed to 1 mg/ml Biotin in egg water. Cryosections were probed with labeled streptavidin and images taken using identical parameters. In Cmo injected embryos, although some background staining for streptavidin was observed (a), only little biotin diffusion was detected (b). In 40% of the *tjp3/zo-3* morpholino injected embryos, a significant accumulation of biotin was observed in the segmentation cavity between the blastoderm and the yolk syncytial layer (c, d, arrows), demonstrating a compromised epidermal barrier in embryos lacking Tjp3/Zo-3. (B) Morphant embryos are more sensitive to the toxic heavy metal cadmium as compared to control embryos. Embryos injected with either control morpholino (Cmo) or *tjp3/zo-3* splice morpholino (MO) were dechorionized at 6 hpf and grown in 1× egg water as a negative control or in egg water containing 0.5 mM $CdCl_2$ or 1 mM $CdCl_2$. Significance of differences was established using 2-way analysis of variance. Cmo embryos had a mortality of ~20% after 42 h exposure to low toxicity $CdCl_2$, whereas the mortality of morphants was significantly higher at ~50% ($p<0.01$). At the high cadmium toxicity, Cmo embryos had ~50% mortality and mortality of MO injected embryos was again significantly higher at ~80% ($p<0.05$). Mean and standard error (S.E.M.); $n\geq 20$ per experiment; 3–4 independent experiments. 2-way ANOVA; $p<0.01$. Asterisks indicate statistical significance.

increased permeability to small tracers and enhanced susceptibility to heavy metals in morphants is thus consistent with a compromised epidermal barrier function.

Tjp3/zo-3 morphants are sensitive to osmotic stress and osmotic stress mimics the morphant phenotype

Osmoregulation is critical for freshwater fish that live in a hypo-osmotic environment. Besides the kidneys and the gills, the skin plays a critical role in the adult fish in regulating the exchange of ions and water with the environment (Rombough, 2002). Given the importance of TJs in controlling paracellular ion permeability and the apparent role of Tjp3/Zo-3 in EVL barrier function, we explored the effect of osmotic stress on *tjp3/zo-3* morphants.

To induce osmotic stress, control or morphant embryos were grown in increasing concentrations of physiological salts. The ability of MO injected embryos to survive high salt conditions was significantly reduced compared to either control embryos or embryos coinjected with a zebrafish *tjp3/zo-3* cDNA to rescue the phenotype (Fig. 9A; *t*-tests, $p<0.05$). Importantly, the increased mortality could be directly linked to the *tjp3/zo-3* MO as high salt and high Mg^{2+} concentrations selected against the morphants (Fig. 9B; 2-way ANOVA, $p<0.05$).

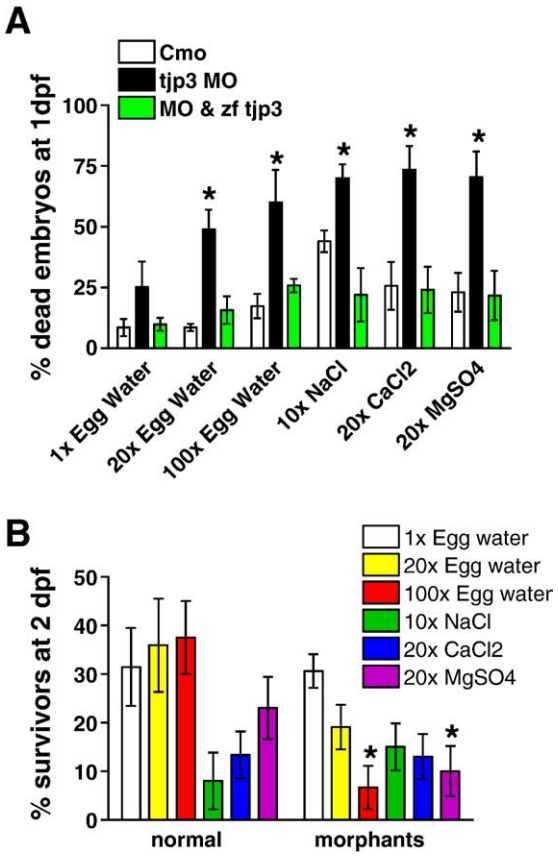

Fig. 9. Tjp3/zo-3 morphants are sensitive to osmotic stress. (A) The ability of *tjp3/zo-3* morphants to survive high salt conditions is significantly reduced compared to control or rescued embryos. Embryos were either injected with control morpholino or *tjp3/zo-3* splice morpholino or they were rescued by coinjecting MO with pcDNA3.1 containing zebrafish *tjp3/zo-3* (MO & zf *tjp3*). Embryos were dechorionized and exposed to high salt conditions (see Materials and methods) at 6 hpf. Surviving embryos were counted at 1 dpf. A significant fraction of *tjp3/zo-3* morpholino injected embryos died prematurely compared to control embryos. Mean and S.E.M.; $n\geq 20$ per experiment; 3–5 independent experiments. *t*-test; $p<0.05$. Asterisks indicate statistical significance. (B) Selection against *tjp3/zo-3* morphants exposed to high salt or high magnesium during embryogenesis. High sodium and calcium salt concentrations reduced the survival of both normal (no phenotype) and morphant embryos. However, in 100× egg water and in 20× MgSO4 the number of morphants that survived to 2 dpf was significantly lower than that of normal embryos. Mean and S.E.M.; $n\geq 20$ per experiment; 3–5 independent experiments. 2-way ANOVA; $p<0.05$; statistical significance is indicated by asterisks.

Due to the hypo-osmotic environment of egg water, a defect in the epidermal barrier function is expected to result in passive water influx, which, if it exceeds the volume that can be cleared by the kidneys, will accumulate in the pericardium and cause edema. Transfer of such embryos from normal egg water into an iso- or hyper-osmotic sucrose solution to dissipate the osmotic gradient alleviates edema, whereas normal embryos die of dehydration (Hentschel et al., 2005). Indeed, ~80% of the *tjp3/zo-3* morphants present with pericardial edema (Fig. 4A). While the incidence of edema of 2 dpf *tjp3/zo-3* morphants selected for phenotypes (i.e. edema, curved tail, small tail fin) placed in egg water did not change over a 24 hr period, a significant decrease was observed in a hyperosmotic sucrose solution (Fig. 10A; 2-way ANOVA, $p<0.01$). The lower incidence of edema was not due to an increased mortality, as their mortality rate was similarly low as that for control embryos until 3 dpf (Fig. 10B).

Intriguingly, we observed that WT embryos grown in high salt conditions frequently developed abnormalities that showed a striking similarity to the *tjp3/zo-3* morphant phenotype, including a small tail fin and, by 48–56 hpf, defects in circulation leading to the accumulation of red blood cells in the tail region (Fig. 10C). This observation indicates that tipping the osmotic balance, either due to osmotic stress or a compromised epidermal barrier, results in similar phenotypic effects on embryos.

Discussion

In the present study we explored the role of the TJ adaptor protein Tjp3/Zo-3 in the developing zebrafish embryo using a morpholino knock down approach. The major phenotypes of the morphant embryos are edema, loss of blood circulation and tail fin malformations. Silencing of *tjp3/zo-3* results in the disruption of the ultrastructure of TJs of the EVL, without affecting cell polarity. Morphants show a loss of epidermal barrier function, as assessed by an increased permeability of the EVL to low molecular tracers and a higher sensitivity of the embryos to osmotic stress.

During mouse development, TJP1/ZO-1 is incorporated into sites of cell–cell adhesion mediated by E-cadherin at the compacted 8-cell embryonic stage (Fleming et al., 2000). TJs

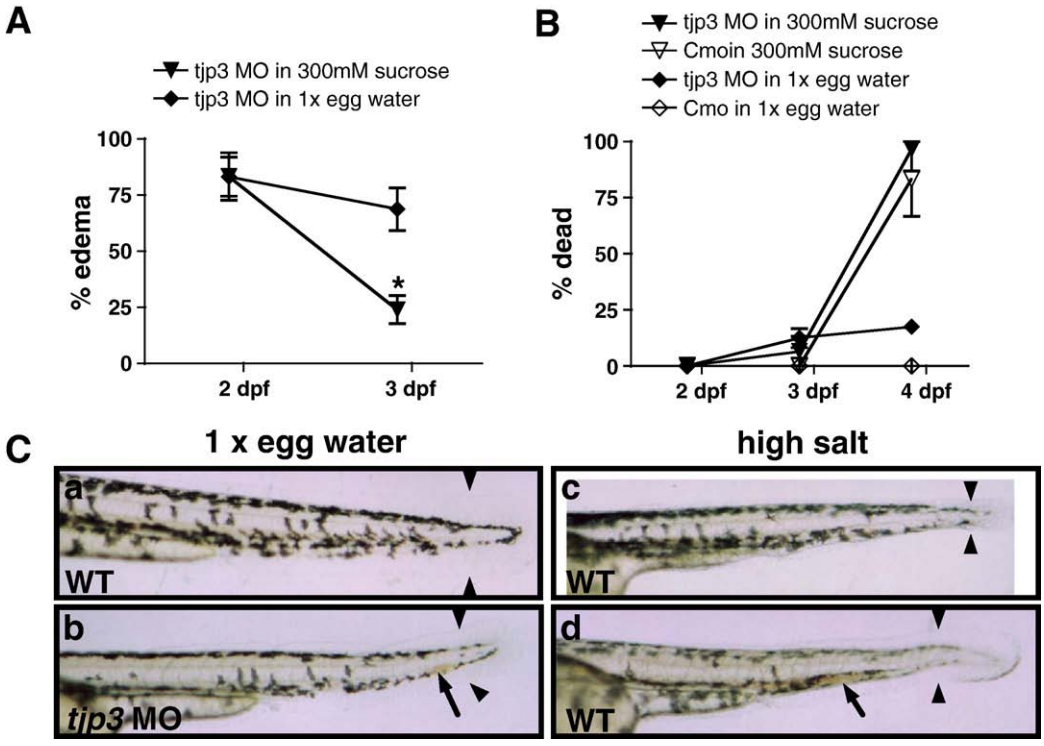

Fig. 10. Compromised osmotic homeostasis mimics the *tjp3/zo-3* morphant phenotype. (A) Pericardial edema of *tjp3/zo-3* morphants can be reversed by growing the embryos in a hyperosmotic sucrose solution. At 2 dpf *tjp3/zo-3* morphants were transferred into a 300 mM sucrose solution. ~80% of *tjp3/zo-3* morphants presented with edema (~20% had a curved tail only). If grown in 1× egg water (diamonds), the incidence of edema only slightly decreased, due to individuals that died. However, if *tjp3/zo-3* morphants were grown in 300 mM Sucrose (triangles), edema incidence dropped significantly. Mean and S.E.M.; $n \geq 10$ per experiment; 5–6 independent experiments. 2-way ANOVA; $p<0.01$. (B) Mortality of embryos grown in 300 mM sucrose. Morpholino injected embryos grown in 1× egg water had a mortality of only ~20% at 4 dpf (diamonds), whereas the mortality for controls was very low (open diamonds). Placed in a hyperosmotic sucrose solution at 2 dpf, most morpholino injected (triangles) and control (open triangles) embryos survived up to 3 dpf, when edema incidence was counted. However, after 48 h exposure close to 90% of both control and morphant embryos died. There was no statistical significance between mortality of control or morphant embryos in 300 mM sucrose. Mean and S.E.M.; $n \geq 10$ per experiment; 2–6 independent experiments. Two-way ANOVA; $p>0.5$. (C) Exposure of WT embryos to high salt conditions mimics the *tjp3/zo-3* morphant phenotype. WT embryos in 1× egg water have a straight tail, a wide tailfin and circulating blood (a). *Tjp3/zo-3* morphants in 1× egg water presented with curved tail, reduced tailfin (b, arrowheads), the loss of blood circulation and an accumulation of red blood cells (b, arrow). 10–15% of control embryos raised in 100× egg water (c), 20× $MgSO_4$ (d), 10× NaCl or 20× $CaCl_2$ (data not shown), also presented with reduced tailfin (c, d, arrowheads), no blood circulation and accumulation of red blood cells (d, arrow).

then mature by the incorporation of the TJP1/ZO-1 a+-isoform, cingulin and rab13 and segregation of the TJ components from the lateral AJs to establish a permeability barrier around the 32-cell stage (Fleming et al., 1993). In the Xenopus embryo, establishment of the permeability barrier is controversial and has been reported to occur as early as the 2-cell stage (Fesenko et al., 2000) or as late as the 64-cell stage (Merzdorf et al., 1998). In the zebrafish, Tjp1/Zo-1 is present in cell–cell junctions of the 8-cell stage embryo. The incorporation of TJP3/ZO-3 has not been analyzed in mouse or Xenopus. Tjp3/Zo-3 is first detected at the 64-cell stage in zebrafish, consistent with a late role in the functional maturation of TJs.

After implantation of the mouse embryo, TJP1/ZO-1 is restricted to the trophectoderm and absent from the inner cell mass (Collins et al., 1995). The trophectoderm forms a permeability barrier between the developing embryo and the uterine environment. In the zebrafish, an analogous function can be attributed to the EVL, which shields the embryo from the aquatic environment (Kimmel et al., 1990). Besides *tjp3/zo-3*, which is highly expressed in the EVL, additional TJ components such as *tjp1/zo-1* and *tjp2/zo-2* (data not shown) are expressed in this cell layer. In addition to its localization to sites of cell–cell contact in the EVL, Tjp3/Zo-3 was also detected in the nucleus at 6 hpf. The relevance of this nuclear localization is not clear since, in contrast to the other two Tjps, Tjp3/Zo-3 has not been linked to any nuclear activity so far. The presence of bona fide TJs in the EVL is evident from the presence of typical electron dense plaques at the luminal end of the lateral membrane of adjoining cells as observed by TEM.

The physiological role of TJP3/ZO-3 has recently been explored by inactivating the corresponding gene in mice (Adachi et al., 2006; Xu et al., 2008). Surprisingly, *TJP3/ZO-3* knock-out mice lack an apparent phenotype, indicating that in mammals TJP3/ZO-3 is dispensable. In contrast, silencing of *tjp3/zo-3* in zebrafish embryos using morpholinos results in a well-defined and specific phenotype. Zebrafish *tjp3/zo-3* but, interestingly, not canine TJP3/ZO-3 rescued the phenotype. This may reflect a unique function of the *tjp3/zo-3* splice variant predominantly expressed in zebrafish embryos, which differs in its domain organization from mammalian TJP3/ZO-3 (Kiener et al., 2007).

The structural integrity of TJs in the EVL of morphants is compromised based on discontinuities and the absence of electron dense junctional plaques. Nevertheless, Tjp1/Zo-1 localization is not dramatically altered and silencing of *tjp3/zo-3* does not affect cell polarity as assessed by the intact asymmetrical distribution of apical and basolateral marker proteins in cells of the EVL and the kidney. Establishing epithelial cell polarity requires the Crumbs complex, containing Crumbs, Pals1 and PATJ (Margolis and Borg, 2005). Silencing of PATJ in tissue culture cells results in the basolateral mislocalization of several TJ proteins, including TJP3/ZO-3 and occludin, a delay in TJ formation and defects in cell polarization (Michel et al., 2005; Roh et al., 2003). The C-terminal PDZ-binding motif in TJP3/ZO-3 interacts with a PDZ domain in PATJ, thereby linking the Crumbs complex to TJs (Roh et al., 2002). The finding that both WT zebrafish Tjp3/Zo-3 and a mutant lacking the C-terminal PDZ-binding motif rescue the morphant phenotypes indicates that these are not due to the inability of Crumbs to link to TJs and is consistent with the intact cell polarity of the morphants. Furthermore, the mutant Tjp3/Zo-3 lacking the C-terminal PDZ-binding motif showed a similar subcellular localization in cells of the EVL and pronephric duct as the WT protein and, as assessed by RT-PCR, the loss of Tjp3/Zo-3 was not compensated by overexpression of components of the Crumbs complex in morphant embryos (data not shown).

Several lines of evidence revealed defects in the barrier function of the EVL of *tjp3/zo-3* morphant embryos. These include the increased permeability of the EVL to small molecules and a higher sensitivity of embryos to toxic heavy metals and osmotic stress. Given the critical role of members of the claudin protein family in forming the TJ permeability barrier and the role of ZO proteins in linking claudins to the underlying cytoskeleton (Tsukita and Furuse, 2000; Van Itallie and Anderson, 2006), our data indicates that tjp3/zo-3 in zebrafish is critical for the ability of claudins in the EVL to establish a functional TJ barrier. At least 25 distinct claudin genes are expressed in the skin of teleosts (Loh et al., 2004). Due to the importance for the interaction of Claudin-16 with ZO-1 for its localization to TJs (Muller et al., 2003), it would be of interest to determine if any of the claudins in the EVL of *tjp3/zo-3* morphants are mislocalized. Unfortunately, such an analysis is currently not feasible because of both the large number of different claudin genes present in teleosts and the lack of antibodies. In this context, it is of interest to note that, reminiscent of the claudinj zebrafish mutant (Hardison et al., 2005), *tjp3/zo-3* morphants show a reduction of otholiths (Fig. 3b).

Pericardial edema and arrest of blood circulation, as observed in the *tjp3/zo-3* morphants, are consistent with defects in osmoregulation and commonly observed if fish are exposed to toxins that impair fluid homeostasis by targeting either the kidney (Hentschel et al., 2005) or the skin (Hill et al., 2004). Edema incidence in *tjp3/zo-3* morphant embryos dropped significantly when the osmotic gradient that drives water influx into the embryo was dissipated. Adult fish rely on the kidneys, the gills and the skin for maintaining ion and water balance. Renal excretion is the primary means to eliminate surplus water before the development of functional gills (Rombough, 2002). Prior to the onset of glomerular filtration, which in zebrafish embryos starts as early 48 hpf (Drummond et al., 1998), the EVL barrier likely plays a key role in osmoregulation (Keller and Trinkaus, 1987).

In conclusion, silencing *tjp3/zo-3* leads to tail fin malformations, pericardial edema and arrest of blood circulation in zebrafish embryos. These phenotypes are a consequence of the compromised osmoregulation and linked to the loss of the permeability barrier of the EVL. Thus Tjp3/Zo-3 is a component of TJs of the EVL of zebrafish embryos and is critical for the function of the EVL as a diffusion barrier.

Acknowledgments

We thank Jovienne Ee Phei San and Nicole Tsang Ying Hung for excellent technical assistance, all members of the Zebrafish

scientific community at IMCB, in particular Vladimir Korzh and Steven Haw Tien Fong, as well as the staff of the IMCB Zebrafish facility for their support, helpful discussions and expert assistance. This work was supported by the Agency for Science, Technology and Research (A*STAR), Singapore.

Appendix A. Supplementary data

Supplementary data associated with this article can be found, in the online version, at doi:10.1016/j.ydbio.2007.12.047.

References

Adachi, M., et al., 2006. Normal establishment of epithelial tight junctions in mice and cultured cells lacking expression of ZO-3, a tight-junction MAGUK protein. Mol. Cell. Biol. 26, 9003–9015.

Anderson, J.M., et al., 2004. Setting up a selective barrier at the apical junction complex. Curr. Opin. Cell Biol. 16, 140–145.

Collins, J.E., et al., 1995. Regulation of desmocollin transcription in mouse preimplantation embryos. Development 121, 743–753.

Drummond, I.A., et al., 1998. Early development of the zebrafish pronephros and analysis of mutations affecting pronephric function. Development 125, 4655–4667.

Fesenko, I., et al., 2000. Tight junction biogenesis in the early Xenopus embryo. Mech. Dev. 96, 51–65.

Fleming, T.P., et al., 1993. Localisation of tight junction protein cingulin is temporally and spatially regulated during early mouse development. Development 117, 1135–1144.

Fleming, T.P., et al., 2000. Assembly of tight junctions during early vertebrate development. Semin. Cell Dev. Biol. 11, 291–299.

Furuse, M., et al., 2002. Claudin-based tight junctions are crucial for the mammalian epidermal barrier: a lesson from claudin-1-deficient mice. J. Cell Biol. 156, 1099–1111.

Gonzalez-Mariscal, L., et al., 2000. MAGUK proteins: structure and role in the tight junction. Semin. Cell Dev. Biol. 11, 315–324.

Gonzalez-Mariscal, L., et al., 2003. Tight junction proteins. Prog. Biophys. Mol. Biol. 81, 1–44.

Hardison, A.L., et al., 2005. The zebrafish gene claudinj is essential for normal ear function and important for the formation of the otoliths. Mech. Dev. 122, 949–958.

Hauptmann, G., Gerster, T., 1994. Two-color whole-mount in situ hybridization to vertebrate and Drosophila embryos. Trends Genet. 10, 266.

Hentschel, D.M., et al., 2005. Acute renal failure in zebrafish: a novel system to study a complex disease. Am. J. Physiol.: Renal. Physiol. 288, F923–F929.

Hill, A.J., et al., 2004. Water permeability and TCDD-induced edema in zebrafish early-life stages. Toxicol. Sci. 78, 78–87.

Keller, R.E., Trinkaus, J.P., 1987. Rearrangement of enveloping layer cells without disruption of the epithelial permeability barrier as a factor in Fundulus epiboly. Dev. Biol. 120, 12–24.

Kiener, T.K., et al., 2007. Identification, tissue distribution and developmental expression of tjp1/zo-1, tjp2/zo-2 and tjp3/zo-3 in the zebrafish, *Danio rerio*. Gene Expression Patterns 7, 767–776.

Kimmel, C.B., et al., 1990. Origin and organization of the zebrafish fate map. Development 108, 581–594.

Kimmel, C.B., et al., 1995. Stages of embryonic development of the zebrafish. Dev. Dyn. 203, 253–310.

Konishi, T., et al., 2006. Enhancing the tolerance of zebrafish (*Danio rerio*) to heavy metal toxicity by the expression of plant phytochelatin synthase. J. Biotechnol. 122, 316–325.

Loh, Y., et al., 2004. Extensive expansion of the Claudin gene family in the teleost fish, Fugu rubripes. Genome Res. 14, 1248–1257.

Margolis, B., Borg, J.P., 2005. Apicobasal polarity complexes. J. Cell. Sci. 118, 5157–5159.

Matter, K., Balda, M.S., 2007. Epithelial tight junctions, gene expression and nucleo-junctional interplay. J. Cell. Sci. 120, 1505–1511.

McNeil, E., et al., 2006. Zonula occludens-1 function in the assembly of tight junctions in Madin–Darby canine kidney epithelial cells. Mol. Biol. Cell 17, 1922–1932.

Merzdorf, C.S., et al., 1998. Formation of functional tight junctions in Xenopus embryos. Dev. Biol. 195, 187–203.

Michel, D., et al., 2005. PATJ connects and stabilizes apical and lateral components of tight junctions in human intestinal cells. J. Cell. Sci. 118, 4049–4057.

Muller, D., 2003. A novel claudin 16 mutation associated with childhood hypercalciuria abolishes binding to ZO-1 and results in lysosomal mistargeting. Am. J. Hum. Genet. 73, 1293–1301.

Roh, M.H., et al., 2002. The carboxyl terminus of zona occludens-3 binds and recruits a mammalian homologue of discs lost to tight junctions. J. Biol. Chem. 277, 27501–27509.

Roh, M.H., et al., 2003. The Crumbs3–Pals1 complex participates in the establishment of polarity in mammalian epithelial cells. J. Cell. Sci. 116, 2895–2906.

Rombough, P., 2002. Gills are needed for ionoregulation before they are needed for O(2) uptake in developing zebrafish, *Danio rerio*. J. Exp. Biol. 205, 1787–1794.

Tsukita, S., Furuse, M., 2000. Pores in the wall: claudins constitute tight junction strands containing aqueous pores. J. Cell Biol. 149, 13–16.

Tsukita, S., et al., 2001. Multifunctional strands in tight junctions. Nat. Rev., Mol. Cell Biol. 2, 285–293.

Umeda, K., 2004. Establishment and characterization of cultured epithelial cells lacking expression of ZO-1. J. Biol. Chem. 279, 44785–44794.

Umeda, K., et al., 2006. ZO-1 and ZO-2 independently determine where claudins are polymerized in tight-junction strand formation. Cell 126, 741–754.

Van Itallie, C.M., Anderson, J.M., 2006. Claudins and epithelial paracellular transport. Annu. Rev. Physiol. 68, 403–429.

Xu, J., et al., in press. Early embryonic lethality of mice lacking ZO-2, but not ZO-3, reveals critical and non-redundant roles for individual ZO proteins in mammalian development. Mol. Cell. Biol. doi:10.1128/MCB.00891-07.